

The Nature of the $X(2175)$ *

S. COITO*, G. RUPP

Centro de Física das Interações Fundamentais, Instituto Superior Técnico,
Technical University of Lisbon, P-1049-001 Lisboa, Portugal

AND

E. VAN BEVEREN

Centro de Física Computacional, Departamento de Física, Universidade de
Coimbra, P-3004-516 Coimbra, Portugal

We study the puzzling vector meson $X(2175)$ in a multichannel generalisation of the Resonance-Spectrum-Expansion model. Besides the usual P -wave pseudoscalar–pseudoscalar, pseudoscalar–vector, and vector–vector channels that couple to mesons with vector quantum numbers, we also include the important S -wave vector–scalar, pseudoscalar–axial-vector and vector–axial-vector channels, including the observed $\phi(1020)f_0(980)$ decay mode. The strong coupling to nearby S -wave channels originates dynamically generated poles, two of which come out close to the energy region of the $X(2175)$, viz. at $(2.037 - i0.170)$ GeV and $(2.382 - i0.20)$ GeV. Further improvements are proposed.

PACS numbers: 14.40.Cs, 11.80.Gw, 11.55.Ds, 13.75.Lb

1. Introduction

The $X(2175)$ was first observed by BABAR [1] in the process $e^+e^- \rightarrow \phi(1020)f_0(980)$, and identified as a 1^{--} resonance, with $M = (2.175 \pm 0.010 \pm 0.015)$ GeV and $\Gamma = (58 \pm 16 \pm 20)$ MeV. This state was then confirmed by BES and denoted $Y(2175)$ [2], from the decay $J/\Psi \rightarrow \eta\phi f_0(980)$, with $M = (2.186 \pm 0.010 \pm 0.006)$ GeV and $\Gamma = (65 \pm 25 \pm 17)$ MeV. It is now included in the PDG Particle Listings [3] as the $\phi(2170)$.

On the theoretical side, the $X(2175)$ has been described as a three-meson resonance in a Faddeev calculation for the $\phi K \bar{K}$ system [4], obtaining a

* Talk at Workshop “*Excited QCD*”, Zakopane, Poland, 8–14 Feb. 2009

narrow peak around 2150 MeV, about 27 MeV wide. Earlier, a conventional Resonance-Chiral-Perturbation-Theory calculation [5] failed to produce such a peak, which led to the former 3-body model. Other approaches include QCD-sum-rule calculations for a tetraquark state [6], and a perturbative multichannel analysis to distinguish between a strangeonium hybrid and a normal 2^3D_1 $s\bar{s}$ state [7].

2. Resonance Spectrum Expansion and the $X(2175)$

In the present study of the $X(2175)$, we use the Resonance-Spectrum-Expansion (RSE) model [8] to unitarise a normal $s\bar{s}$ spectrum. In the RSE approach, non-exotic mesons are described as regular quark-antiquark states, but non-perturbatively dressed with meson-meson components. An important feature is the inclusion of a complete $q\bar{q}$ confinement spectrum in the intermediate state [8, 9], resulting for the multichannel case in an effective meson-meson potential

$$V_{ij}^{(L_i, L_j)}(p_i, p'_j; E) = \lambda^2 j_{L_i}^i(p_i a) j_{L_j}^j(p'_j a) \sum_{n=0}^{\infty} \frac{g_i(n) g_j(n)}{E - E_n}, \quad (1)$$

where λ is an overall coupling constant, a a parameter mimicking the average string-breaking distance, $j_{L_i}^i$ a spherical Bessel function, p_i and p'_j the relativistically defined relative momenta of initial channel i and final channel j , respectively, $g_i(n)$ the coupling of channel i to the n -th $q\bar{q}$ recurrence, and E_n the discrete energy of the latter confinement state. Note that the couplings $g_i(n)$, evaluated on a harmonic-oscillator (HO) basis for the 3P_0 model [10], decrease very rapidly for increasing n , so that practical convergence is achieved with the first 20 terms in the infinite sum. Moreover, the separable form of the effective potential (1) allows the solution of the (relativistic) Lippmann-Schwinger equation in closed form.

In the present first study, we restrict ourselves to the 3S_1 channel for the $q\bar{q}$ system. Moreover, we assume ideal mixing, so that only $s\bar{s}$ states are considered. For the confinement mechanism, we take an HO potential. This choice is not strictly necessary, as Eq. (1) allows for any confinement spectrum, but the HO has shown to work fine in practically all phenomenological applications. The flavour-dependent HO spectrum reads

$$E_n = m_q + m_{\bar{q}} + \omega(2n + 3/2 + \ell). \quad (2)$$

The parameter values $\omega = 190$ MeV and $m_s = 508$ MeV are kept unchanged with respect to all previous work (see e.g. Ref. [11]). In Table 1, we list some of the eigenvalues given by Eq. (2). As for the decay sector that couples to $J^{PC}=1^{--}$ ϕ states, we take all pseudoscalar–pseudoscalar (PP),

n	$s\bar{s}$
0	1.301
1	1.681
2	2.061
3	2.441
4	2.821

Table 1. HO eigenvalues (2) in GeV, for $\omega = 190$ MeV, $m_s = 508$ MeV, $\ell = 0$.

pseudoscalar–vector (PV), and vector–vector (VV) channels, which are in P -waves, as well as all vector–scalar (VS), pseudoscalar–axial-vector (PA), and vector–axial-vector (VA) channels, being in S -waves. These 15 channels are listed in Table 2, including the observed $[1, 2]$ $\phi f_0(980)$ mode, with the respective orbital angular momenta, spins, and thresholds.

Channel	Relative L , Total S	Threshold
KK	1, 0	0.987
KK^*	1, 1	1.388
$\eta\phi$	1, 1	1.567
$\eta'\phi$	1, 1	1.977
K^*K^*	1, 0	1.788
K^*K^*	1, 2	1.788
$\phi f_0(980)$	0, 1	1.999
$K^*K_0^*(800)$	0, 1	1.639
$\eta h_1(1380)$	0, 1	1.928
$\eta' h_1(1380)$	0, 1	2.338
$KK_1(1270)$	0, 1	1.764
$KK_1(1400)$	0, 1	1.894
$K^*K_1(1270)$	0, 1	2.164
$K^*K_1(1400)$	0, 1	2.294
$\phi f_1(1420)$	0, 1	2.439

Table 2. Thresholds in GeV of included meson-meson channels (see Ref. [3]).

3. Results

As emphasised above, the T -matrix for the effective potential (1) can be solved in closed form. Bound states and resonances correspond to poles of T on the appropriate sheet of the many-sheeted Riemann surface. For the 15 channels considered, there are $2^{15} = 32,768$ such sheets. However, the relevant poles are in principle those that correspond to relative momenta with negative imaginary parts with respect to open channels, and positive

imaginary parts for closed channels. The simplest example of a latter-type pole is a bound state, for which the real part of the momentum is zero.

The only two free parameters of the model, viz. λ and a , we fix by demanding that the mass and width of the $\phi(1020)$ be reasonably reproduced. For $a = 5.0 \text{ GeV}^{-1}$ and $\lambda = 3.75 \text{ GeV}^{-3/2}$ we get a theoretical pole position of $E_{\text{theor}} = (1.0145 - i0.0034) \text{ GeV}$, to be compared with the PDG [3] value $E_{\text{exp}} = (1.0195 - i0.0021) \text{ GeV}$, which is more than good enough for the present simplified investigation. Of course, besides the $\phi(1020)$, there are several other resonance poles, which are given in Table 3, for energies up to about 2.5 GeV^1 . Confinement poles are those that

Re	Im	Type of Pole
1.0145	-0.0034	confinement, $n = 0$
1.457	-0.011	confinement, $n = 1$
1.980	-0.010	confinement, $n = 2$
2.037	-0.170	continuum
2.382	-0.020	continuum
2.580	-0.123	continuum

Table 3. Pole positions, in GeV.

end up at the energies of the confinement spectrum in the limit $\lambda \rightarrow 0$. These usually have small to moderate imaginary parts. On the other hand, the continuum poles, which are dynamically generated, disappear in the complex energy plane for $\lambda \rightarrow 0$, with $\text{Im}E \rightarrow -\infty$. The latter poles mostly have large imaginary parts, for physical values of λ , but there are exceptions, like the fifth pole in Table 3. Typical cases of pole trajectories are shown in Fig. 1, with the $n = 2$ confinement pole in the left-hand plot and the first continuum pole in the right-hand one. The jump in the trajectory of the confinement pole is due to a change of Riemann sheet at the $\phi f_0(980)$ threshold. The trajectory of the second continuum pole is depicted in Fig. 2, left-hand plot, which shows its highly non-linear and non-perturbative behaviour. As for the main purpose of the present work, we find two poles in the energy region 2.0–2.4 GeV relevant for the $X(2175)$, namely at $(2.037 - i0.170) \text{ GeV}$ and $(2.382 - i0.020) \text{ GeV}$, being both continuum poles. The 4^3S_1 ($n=3$) confinement pole can be easily followed from $E = 2.441 \text{ GeV}$, up to a value of $\lambda \approx 3.1 \text{ GeV}^{-3/2}$, but one loses its track when switching Riemann sheet at the opening of the $\phi f_1(1420)$ channel. In any case, all these precise pole positions are not so important for this first study. Suffice it to say that dynamical poles can be generated in the energy region pertinent to the $X(2175)$, and possibly with quite small

¹ These results are slightly different from the preliminary ones presented at the workshop, due to a, now corrected, minor error in the computer code.

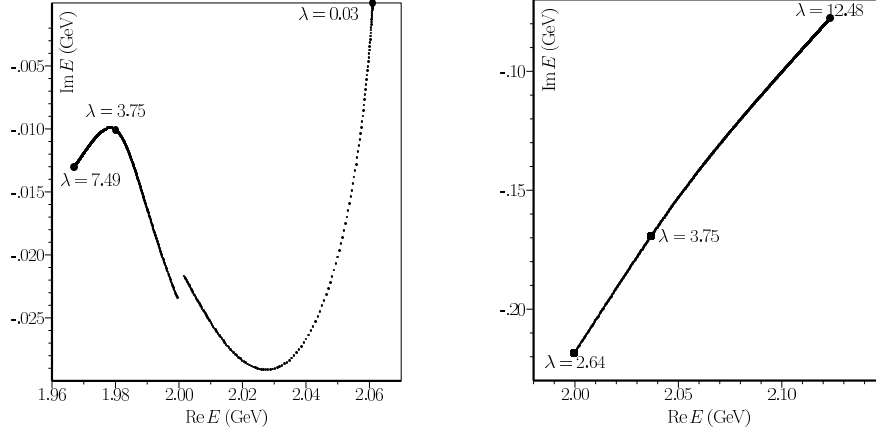


Fig. 1. Confinement pole for 3^3S_1 state (left); first continuum pole (right).

imaginary parts. Preliminary results for a more complete calculation [12], including the 3D_1 states, indicate a considerable improvement of the pole positions for the $X(2175)$ candidates.

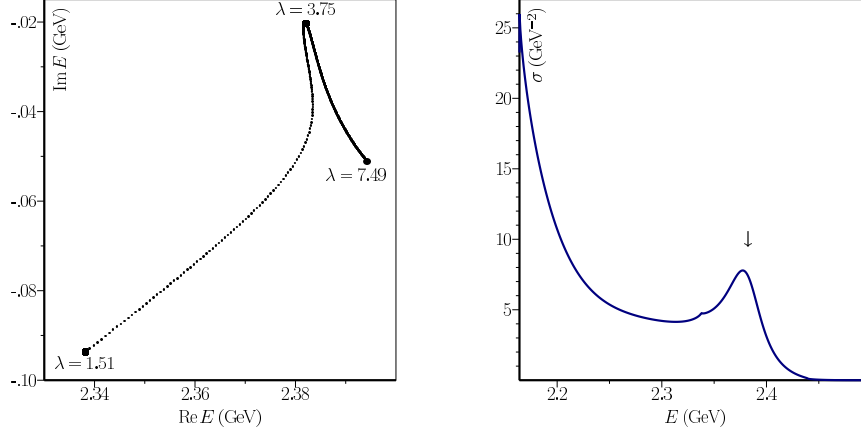


Fig. 2. Second continuum pole (left); elastic $K^*K_1(1270)$ cross section (right).

Having the exact T -matrix at our disposal, we can easily compute observables, too, like cross sections and phase shifts. Although this is not of great importance here, in view of the rather tentative pole positions above 2 GeV, we show in Fig. 2, right-hand plot, the S -wave $K^*K_1(1270)$ cross section, just as an illustration. The pole at $(2.382 - i0.020)$ GeV is clearly visible here, in contrast with the $\phi f_0(980)$ channel. Inclusion of the 3D_1 states turns out to significantly improve the description, both for the pole positions and for the $\phi f_0(980)$ cross section [12], in line with experiment.

4. Conclusions and outlook

We have shown that coupling a spectrum of confined $s\bar{s}$ states to all S -wave and P -wave two-meson channels composed of light mesons allows to generate dynamical resonances above 2 GeV, besides roughly reproducing the mass and the width of the $\phi(1020)$. This may provide a framework to understand the puzzling $X(2175)$ meson, owing to the large and non-linear coupled-channel effects, especially from the S -wave channels. Inclusion of the 3D_1 $s\bar{s}$ states will then account for a more realistic modelling, as confirmed by preliminary results [12]. Further improvements may be considered as well, such as deviations from ideal mixing, smearing out resonances in the final state, and more general transition potentials.

Acknowledgements

We thank the organisers for an inspiring and pleasant workshop. We are also indebted to K. Khemchandani for very useful discussions. This work was supported in part by the *Fundação para a Ciência e a Tecnologia* of the *Ministério da Ciência, Tecnologia e Ensino Superior* of Portugal, under contract CERN/FP/83502/2008.

REFERENCES

- [1] B. Aubert *et al.* [BABAR Collaboration], Phys. Rev. D **74** (2006) 091103.
- [2] M. Ablikim *et al.* [BES Collaboration], Phys. Rev. Lett. **100** (2008) 102003.
- [3] C. Amsler *et al.* [Particle Data Group], Phys. Lett. B **667** (2008) 1.
- [4] A. Martinez Torres, K. P. Khemchandani, L. S. Geng, M. Napsuciale and E. Oset, Phys. Rev. D **78** (2008) 074031.
- [5] M. Napsuciale, E. Oset, K. Sasaki and C. A. Vaquera-Araujo, Phys. Rev. D **76** (2007) 074012.
- [6] Z. G. Wang, Nucl. Phys. A **791** (2007) 106; H. X. Chen, X. Liu, A. Hosaka and S. L. Zhu, Phys. Rev. D **78** (2008) 034012.
- [7] G. J. Ding and M. L. Yan, Phys. Lett. B **657** (2007) 49.
- [8] E. van Beveren and G. Rupp, Int. J. Theor. Phys. Group Theor. Nonlin. Opt. **11** (2006) 179.
- [9] E. van Beveren and G. Rupp, Annals Phys., in press, DOI 10.1016/j.aop.2009.03.013 [arXiv:0809.1149 [hep-ph]].
- [10] E. van Beveren, Z. Phys. C **21** (1984) 291.
- [11] E. van Beveren, G. Rupp, T. A. Rijken and C. Dullemond, Phys. Rev. D **27** (1983) 1527.
- [12] S. Coito, E. van Beveren and G. Rupp, in preparation.